

Calculations of energies for self-diffusion in n-alkanes

B. L. Farmer

Mechanical and Materials Engineering, Washington State University, Pullman, WA 99164-2720, USA

and R. K. Eby

Materials Science and Engineering, The Johns Hopkins University, Baltimore, MD 21218, USA

(Received 30 August 1986)

Calculations for diffusion in orthorhombic, monoclinic and triclinic subcells are reported. They show that self-diffusion can occur and support a vacancy mechanism. Vacancy energies are much larger than the barriers to molecular motion. Diffusion parallel to the basal plane can be by a rigid rod mechanism while perpendicular requires a conformational jog to traverse the crystal boundary. The diffusion coefficients are in order of magnitude agreement with the limited experimental data available. For a given subcell, diffusion parallel to the basal plane is about an order of magnitude greater than perpendicular. Diffusion coefficients for the triclinic subcell are larger than those in the other two. The computed coefficients are especially sensitive to some of the parameters used.

(Keywords: n-alkanes; barriers; calculations; energies; self-diffusion; vacancies)

INTRODUCTION

Self-diffusion has an important influence upon relaxations, recrystallization, crystal perfection and other characteristics of the crystals of alkanes as well as polyethylene. Measurements with tracers have shown rather directly that self-diffusion can occur parallel to the basal plane in n-eicosane single crystals¹ and in polyethylene single crystals after the folds have been removed with nitric acid². Neutron quasi-elastic scattering has shown such diffusion in n-tricosane³, but not in n-tritriacontane^{4,5}. There have been many demonstrations of self-diffusion perpendicular to the basal plane in alkanes, other small molecules and polyethylene¹⁻⁹. In this article we report calculations which we made some time ago^{10,11} for the energies involved in self-diffusion of n-alkanes by the migration of row vacancies.

COMPUTATIONAL METHOD AND MODEL

Vacancy migration

In closely packed alkane and polyethylene crystals molecular interstitials would be expected to have very high defect energies. Vacancies, on the other hand, have been shown to have energies equal to that which a molecule would have, were it to occupy the vacancy in the crystal¹². Thus, it has been accepted that self-diffusion would proceed by vacancy rather than interstitial migration¹. This is supported by the fact that the activation enthalpy for self-diffusion is indeed of the order of the heat of sublimation (i.e. the energy of a vacancy) for a number of molecular crystals^{1,6,13}. If vacancy

migration is assumed to be the mechanism of self-diffusion, the energy of the vacancy strongly affects the diffusion. Since vacancy energies have not been reported previously, they will be calculated for the crystals of interest.

Diffusion parallel to the basal plane

Another factor affecting the diffusion is the energy barrier to vacancy motion; that is, the energy barrier which an adjacent molecule must surpass in order to fill the vacancy and leave the vacancy at a new substitutional site. One can imagine intramolecular twisting or rotating mechanisms by which a long, flexible molecule can translate parallel to the basal plane to fill a vacancy in a segmental manner. However, for sufficiently short alkanes, the energies should favour primarily a rigid rod motion of the molecule. Some experimental data on molecular motions can be interpreted in this manner^{9,14}. Calculations have not been reported previously. Therefore, these first calculations of the barrier are made for a rigid molecule undergoing the translation and rotation necessary to translate to an adjacent vacant site in crystals of interest. As a consequence of this approach, the vacancy energy discussed above is that of a row vacancy equal in length to that of the alkane host.

Diffusion perpendicular to the basal plane

Because of its relevance to relaxations and the annealing of polyethylene crystals, the transport of alkane and polyethylene molecules along their axes has been the subject of much interest. A number of models have been proposed and the barriers to motion have been calculated

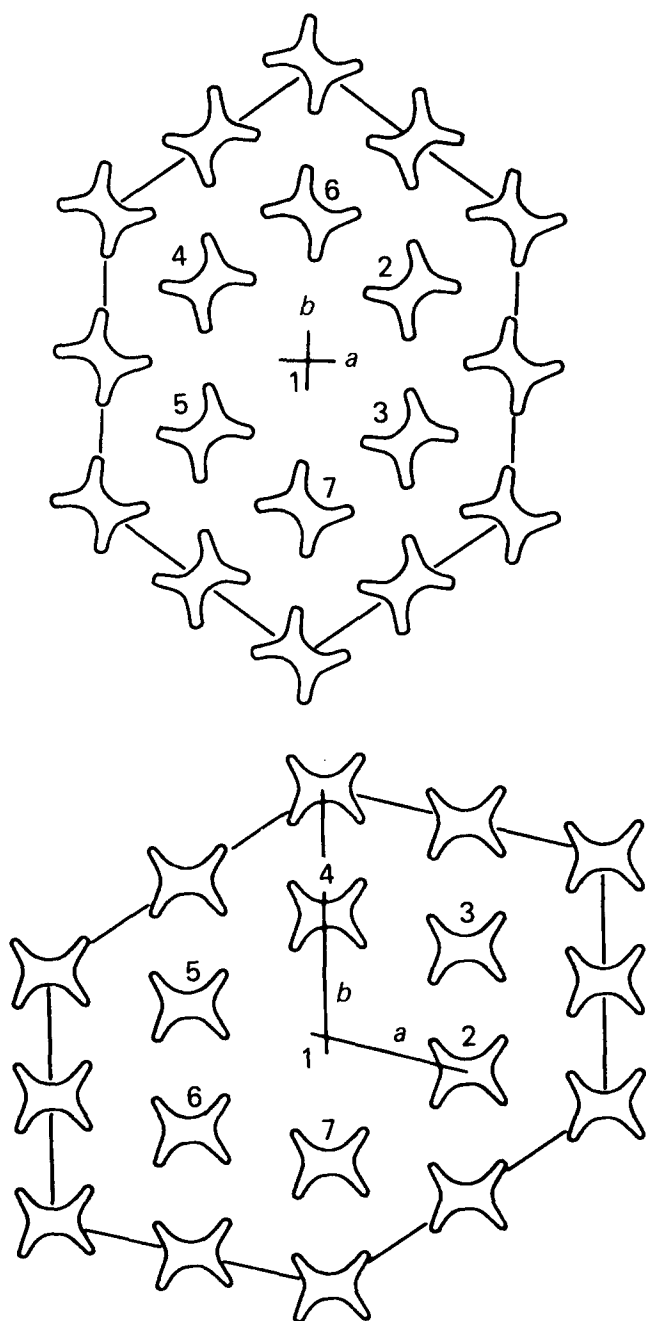


Figure 1 Schematic representations of the basal projection of the 19 chain arrays for the orthorhombic (top) and monoclinic/triclinic (bottom) structures

for both rigid^{15,16} and flexible¹⁷⁻¹⁹ transport of the molecules. For the reasons discussed in the previous section, rigid alkanes will be considered here. Thus, the calculations will be basically the same as those reported previously^{15,16}, but the results will be cast in terms of diffusion parameters and some discussion of kinking will be presented.

Model

The computational method follows that described previously^{16,20}. Chains of eight methylene units in the planar zig-zag conformation were held internally rigid at the bond angles and bond lengths used previously²⁰. The chains were held parallel to one another, and were allowed four degrees of freedom: three translations parallel to the unit cell axes, and rotation about the chain

axis. The position of a chain was defined in terms of the fractional coordinates of the intersection of its chain axis with a planar grid, normal to the chain axis, defined by the a , b and γ unit cell parameters. In the case of the triclinic paraffin packing mode, the grid was defined by the projections of these same parameters onto the plane normal to the chain axes. Initial values for these cell dimensions were those which gave the minimum energy for the perfect crystal. The potential energy parameters of Williams were used²¹. The c dimension was taken as 2.54 Å.

The minimization procedure was also the same as that used previously^{16,20}. A grid search method was employed, using 0.01 increments in the fractional positions f_a and f_b , a 0.05 increment in the fractional position f_c , and a one degree increment for the setting angle. The minimum energy positions and orientations of the chains were always determined sequentially, minimizing one chain at a time, until all had been adjusted. In every case, minimization was carried out in the presence of all appropriate neighbouring chains. Because of the small shifts that were observed in the first cycle of minimization, the second cycle of sequential adjustment, necessary in previous investigations of methyl branches, was omitted. The final step was the adjustment of the unit cell parameters.

The arrays for the calculations of vacancy diffusion in the orthorhombic and monoclinic packing modes are shown in projection on the basal plane in Figure 1. The triclinic mode is identical to that for the monoclinic, differing only in the translations of the chains normal to the plane of projection. Specifically, the triclinic mode has translations of 0.25 and 0.50 (f_c) between neighbouring chain segments in the a and b cell directions, respectively. Interactions between a chain and its close neighbours were considered. An exception to this was necessary in considering the motion of a vacancy in the array (or equivalently, the motion of a chain into a vacancy). In order to avoid a discontinuity in the calculated energy, it was necessary to compute the interactions of the mobile chain with all the chains surrounding both its initial and final positions.

When a vacancy is present, there are six lateral neighbours which potentially can exchange positions with the vacancy. By virtue of symmetry, pairs of these are identical. Therefore, for a vacancy originally located at the positions designated 2, 3 or 7, a chain from the position designated 1 was allowed to diffuse into the vacancy in each type of crystal. These three cases will be denoted as O12, O13 and O17, respectively, in the orthorhombic array, as T12, T13 and T17 in the triclinic array and as M12, M13 and M17 in the monoclinic array. As might be anticipated from the arrangements of the chains shown in Figure 1, cases O13, M13 and T13 were very much higher in energy than the others. They could not be accomplished without substantial enlargement of the arrays at a correspondingly high cost in energy. They were therefore eliminated from further consideration.

To investigate the diffusion of a chain into an adjacent vacancy, the chain was moved stepwise from its initial to its final position along the most direct path with respect to its fractional coordinates. For example, in diffusion case O12, a chain originally at fractional coordinates (0.0,0.0) was moved to coordinates (0.5,0.5) by incrementing both f_a and f_b by 0.05 simultaneously. At each location along this

path, a scan was made of the energy as a function of orientation and f_c position over their full unique ranges, at intervals of 20 degrees and 0.05, respectively. In the same way, for case M17, the f_b coordinate was incremented in steps of -0.10 for a chain originally at position 1 (0.0,0.0) and ending at position 7 (0.0, -1.0). For the triclinic crystal, translation in the c direction was handled in analogous fashion. From these data, energy contour maps were drawn to determine the approximate position of the highest energy point of the diffusion process. This region was then surveyed in smaller disposition increments. In some cases, the contour maps suggested that more than one path might be possible; for example, rotation followed by translation *versus* translation followed by rotation. The energy associated with each likely path was considered.

The saddle-point energies located in this manner correspond to a situation in which the neighbouring chains have not adjusted their dispositions to accommodate the motion of the diffusing chain. They are therefore best viewed as an upper bound of the energy barrier to diffusion. A lower bound was computed by fixing the diffusing chain at its saddle-point disposition, and minimizing the energy by adjusting the dispositions of the neighbouring chains. This relaxation of the array was carried out as described above. When necessary, the array was enlarged beyond the chains shown in *Figure 1* to assure that all the chains involved in interactions with the diffusing one would not be on the edge of the model.

RESULTS AND DISCUSSION

Energies

The excess energies of the row vacancies are given in *Table 1*. It was found that the energy of a vacancy is equal to the total that a molecule in that position would have. This is a consequence of the facts that, during the energy minimization, the molecules surrounding the vacancy exhibited no tendency to shift to delocalize the density deficiency and the overall dimensions of the array did not change. These observations, which did not change as a result of various modifications of the computational procedure, are qualitatively similar to the calculated results for other materials²². As will be seen, these vacancy energies are an important component of the activation energy for self diffusion in alkanes. The energies in column 2 are for a single methylene group in a single alkane crystalline array containing molecules which are eight carbon atoms in length. The energies for a stacked array of such crystals (as in a large octane single crystal) would be a little different because of the end group packing effects which are present at the interface between

lamellar crystals and are not taken into account here²³. Also the calculated energies are a little high because of end effects associated with short molecules used. Therefore, the energies were recalculated for a single methylene unit in the centre of an array large enough to eliminate cut-off effects. These are given in the third column of *Table 1*. They represent the upper limit to the energy for a stacked array of crystals. They agree well with values in the literature and are probably better values than those in column two²³. Note that these energies are twice the lattice energy.

Consider the molecule in site one as it moves parallel to the basal plane to a vacancy at site three of the orthorhombic crystal in *Figure 1*. As discussed above, it can rotate about as well as translate along its axis, and there are many possible paths for it to follow to site three. Therefore, the energy contour maps in *Figure 2* were made to show the energy as a function of setting-angle and axial displacement at nine equally spaced positions between the sites. With these, low-energy paths (with respect to setting angle and axial displacement) to site three were constructed. One such path for this case is shown in *Figure 3*. If the positions of the surrounding molecules at the peak of the barrier are allowed to relax, the energy per methylene group decreases about 0.4 kJ mol^{-1} . In general there were a number of paths with similar energy barriers for each crystal and pair of sites. The lowest energy for each case is given in *Table 2*. These energies are considerably smaller than those given in *Table 1* for vacancy energies and will be correspondingly less important in determining the activation energies for self-diffusion parallel to the basal plane. The energies for a stacked array of such crystals would be slightly different because of interface effects.

The path having the lowest energy barrier for motion of the molecule parallel to its axis was determined in a manner akin to that just described for motion parallel to the basal plane and to that described previously¹⁶. The energies for the unrelaxed and relaxed crystals are given in *Table 3*. As in the case of motion parallel to the basal plane, these numbers are considerably smaller than the vacancy energies. Therefore, the activation energy for diffusion parallel to the molecular axis might also be determined primarily by the vacancy energy. However, there are some other factors that must be considered first. The energies given in *Table 3* are for a single layer crystal. This means that the energies are a little too high for a stacked array of such crystals because of end effects associated with the protrusion from the crystal layer of the molecule that is being moved. On the other hand, the energies are too low for a stacked array because in reality the molecules would have to 'kink' or 'bend' in order to move from one crystal layer to the next. This is a consequence of the fact that the axes of the molecules are not colinear in successive layers of alkane crystals^{24,25}. As noted earlier, the energies associated with such defects have been calculated. They can be significant. Their consequences will be considered in the next section.

Diffusion coefficients

The results above can be used to estimate diffusion coefficients for one-dimensional diffusion along the direction of a single concentration gradient. The following equation applies approximately to that situation as well as to diffusion along the principal axes of

Table 1 Excess energies of vacancies in various crystal structures

Structure of subcell	Energy of a CH ₂ vacancy ^a (kJ mol ⁻¹)	Energy of a CH ₂ vacancy ^b (kJ mol ⁻¹)
Orthorhombic	11.45	15.38
Monoclinic	11.47	15.50
Triclinic	10.77	15.22

^a Calculated from the excess energy for a row vacancy which is eight carbon atoms long and located in the middle of a cluster of nineteen such molecules

^b Calculated from the energy of a CH₂ in the centre of an array of size sufficient to eliminate cut-off effects

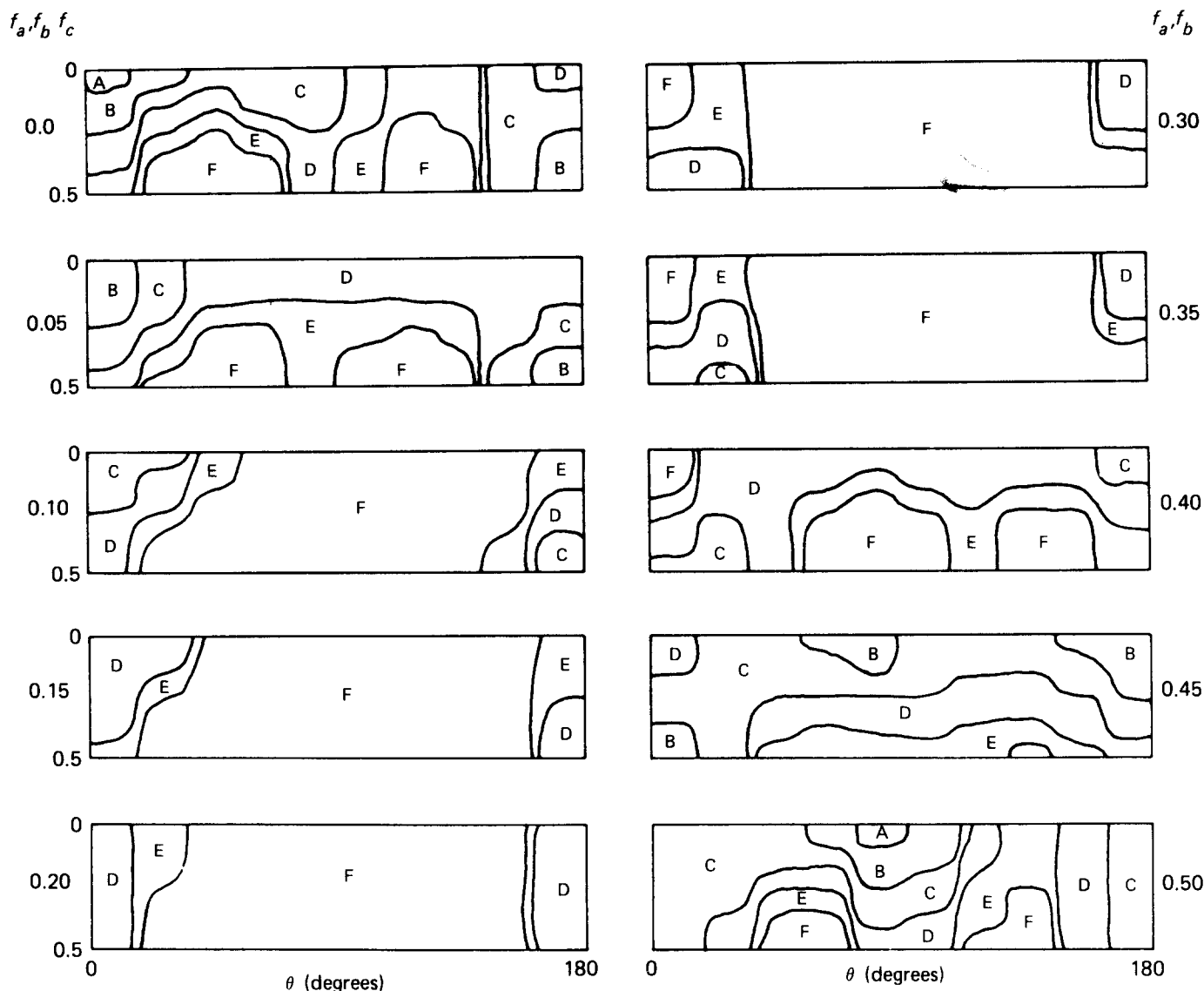


Figure 2 Energy contour maps for translation (f_c) and rotation (θ) for a molecular at position f_a, f_b , enroute from site 1 to site 3 in the orthorhombic environment. Contours are drawn at 1 kJ mol^{-1} of CH_2 relative to the lowest energy (crystallographic) position. Regions are designated as follows: A, 0 to $1 \text{ kJ mol}^{-1} \text{ CH}_2$; B, 1 to $2 \text{ kJ mol}^{-1} \text{ CH}_2$; C, 2 to $3 \text{ kJ mol}^{-1} \text{ CH}_2$; D, 3 to $4 \text{ kJ mol}^{-1} \text{ CH}_2$; E, 4 to $5 \text{ kJ mol}^{-1} \text{ CH}_2$; F, $> 5 \text{ kJ mol}^{-1} \text{ CH}_2$

a crystal with any arrangement of concentration gradients:

$$D = 1/2 f w_0 \sum_{j=1}^Z e^{+(\Delta S_v + \Delta S_{mj})/R} e^{-(\Delta H_v + \Delta H_{mj})/RT} a_j^2 \cos^2 \theta_j \quad (1)$$

Here ΔH_v is the excess enthalpy of a diffusing defect and ΔH_{mj} is the enthalpy barrier to motion (jumps) of a molecule from one site to the j th of Z neighbouring sites. The terms, ΔS_v and ΔS_{mj} , are the corresponding entropies. The jump distance is a_j and the angle between the jump direction and the direction of the concentration gradient is θ_j . At a very high temperature, the jump attempt frequency is w_0 . The correlation factor, f , is related to non-random jumps and has an upper limit of $(1-2/z)$. There are a number of approaches to elements of equation (1) and it is susceptible to a variety of refinements concerning non-random jumps, isotope masses, variable diffusion coefficients, etc.²⁶⁻²⁹. Nevertheless, it is useful to apply it to tracer diffusion for the present crystals.

The energies given in *Tables 1-3* are internal energies. However, they can be taken as enthalpies because the volume changes involved are zero or very small and the pressure is one atmosphere. The enthalpy relevant to the abundance of the vacancies will be taken to be one-half of the values in *Table 1* for the largest array. This is done since the mechanism of vacancy creation is not by sublimation of a molecule but relocation of a molecule to the surface of the crystal to create a new substitutional site. The factor one-half represents an estimate of the energy recovered at the surface by virtue of a displaced molecule remaining in association with the crystal surface. The barrier enthalpies are taken as the unrelaxed values in *Tables 2 and 3*. Since some data are available for diffusion in *n*-eicosane, the various enthalpies are calculated for twenty carbon atoms¹. The entropies are not easy to evaluate directly, but can be estimated by an empirical equation³⁰:

$$\Delta S = 4\alpha \Delta H \quad (2)$$

Here α is the thermal volume expansion coefficient. It

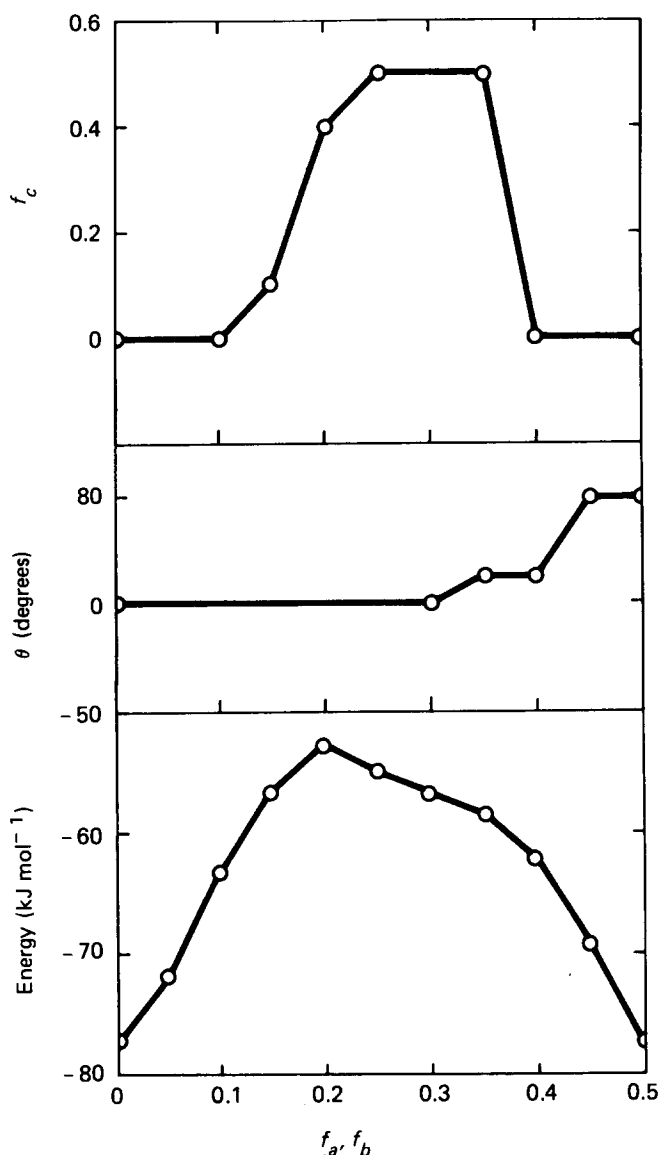


Figure 3 Lowest energy pathway for a molecule moving from site 1 (0,0,0) to site 3 (0.5, 0.5) in an orthorhombic environment. The optimum translation f_c (top), optimum orientation θ (middle) and the corresponding energies (bottom) are shown at the indicated f_a, f_b positions of the molecule which is 8 carbon atoms long

varies with the crystal thickness and can be taken as $6 \times 10^{-4} \text{C}^{-1}$ for C_{20} ^{7,31-34}. The attempt frequency is taken as 3.5×10^{11} , a value which was found suitable in considering molecular relaxations of alkanes¹⁶. The correlation factor is taken as 0.83. Jump distances and angles can be evaluated from the crystal structure since the structure next to a vacancy did not change significantly from that of the perfect crystal. The unit cell parameters are given in Table 4.

For jumps between crystal layers, there are four molecules which are close enough to move into each end of a vacancy^{24,25}. As noted above, each of these must go through a jog or kink in order to make the move. While calculations have not been made for the exact geometry of this situation, they have been made for a number of related models^{17-19,35}. These have yielded a similar range of energies. The value 34 kJ mol^{-1} is used here. There have been fewer calculations of the barrier for the jogs to move along the molecule or, alternatively, for the molecule to move through the jog^{18,19}. The value

17 kJ mol^{-1} is used here. In the selection of these numbers, the different packing environment at the interface of the crystal layers has been considered.

The jogs thus lead to a different enthalpy of activation. The enthalpy at the jog must be added appropriately to the enthalpy of the vacancy since both are required before the jump can occur. Further, the barrier for motion of the molecule through the jog must be added appropriately to the barrier for the carbon atoms not in the jog. Thus, as the molecule begins to move out of the first crystal layer, it will go over a short series of rapidly increasing barriers to sites of rapidly increasing energy as the jog is formed. As the molecule enters the second crystal, it will go over a longer series of approximately constant barriers to a series of states of approximately constant energy. These barriers will be the sum of the barrier to move through the jog and the barrier for the carbon atoms not in the jog to move through the crystal. The energy of the states will be the sum of the vacancy and jog energies. As the tail end of the molecule leaves the first crystal, the process will reverse and the molecule will go over a short series of rapidly decreasing barriers to states of rapidly decreasing energies as the jog is removed.

The situation above presents interesting questions. It is

Table 2 Energy barriers for molecular motion parallel to the basal plane

Structure of subcell	Sites ^a	Unrelaxed barrier for a CH_2^b (kJ mol^{-1})	Relaxed barrier for a CH_2^b (kJ mol^{-1})
Orthorhombic	1,2;1,3	2.67	2.20
Monoclinic	1,2	3.14	2.54
	1,7	1.46	1.28
Triclinic	1,2	2.80	2.30
	1,7	1.29	1.13

^a Numbered according to Figure 1. As noted in the text, symmetry leads to another pair of sites identical in barrier to each of the ones given here. The other possible pairs of sites which are not given here were found to have much greater barriers

^b Calculated from the barrier for a molecule which is eight carbon atoms long and located in a cluster. As described in the text the region near the peak of the curves such as that in Figure 3 were surveyed in finer increments to yield the values here

Table 3 Energy barriers for motion parallel to the molecular axis

Structure of subcell	Unrelaxed barrier for a CH_2^a (kJ mol^{-1})	Relaxed barrier for a CH_2^a (kJ mol^{-1})
Orthorhombic	2.44	1.77
Monoclinic	2.68	2.02
Triclinic	1.76	1.10

^a Calculated from the barrier for a molecule which is eight carbon atoms long and located in the middle of a cluster of nineteen such molecules

Table 4 Unit cell parameters for minimum energy^a

Structure of subcell	<i>a</i> (Å)	<i>b</i> (Å)	α (deg)	β (deg)	γ (deg)
Orthorhombic	7.26	4.94	90	90	90
Monoclinic	4.53	4.08	90	90	104
Triclinic ^b	4.63	4.25	82.1	72.6	107.6

^a As noted in the text the zig-zag repeat was taken at 2.54 Å

^b The triclinic dimensions presume the experimentally observed staggering between molecules

Table 5 Diffusion parameters calculated for *n*-icosane

Structure of subcell	Diffusion direction	A^a ($\text{m}^2 \text{s}^{-1}$)	B^a (kJ mol^{-1})	C^a ($\text{m}^2 \text{s}^{-1}$)	E^a (kJ mol^{-1})	D at 296.7 K ($\text{m}^2 \text{s}^{-1}$)
Orthorhombic	<i>a</i>	4.8×10^{18}	207	0	0	2.7×10^{-18}
	<i>b</i>	2.2×10^{18}	207	0	0	1.3×10^{-18}
	$\perp ab$	7.0×10^{22}	235	0	0	5.5×10^{-19}
Monoclinic	<i>a</i>	8.3×10^{19}	218	2.5×10^{14}	184	2.1×10^{-18}
	<i>b</i>	4.9×10^{18}	218	4.2×10^{15}	184	2.5×10^{-17}
	$\perp ab$	2.9×10^{23}	240	0	0	3.1×10^{-19}
Triclinic	<i>a</i> ^b	4.9×10^{18}	208	6.9×10^{13}	178	7.0×10^{-18}
	<i>b</i> ^b	4.5×10^{17}	208	7.6×10^{14}	178	5.6×10^{-17}
	$\perp ab$	3.6×10^{21}	225	0	0	1.6×10^{-18}

^a Parameters for equation (3) in the text^b In these cases, a third set of parameters which take account of the contributions from diffusion along the molecular axis are negligible

akin to multiple site relaxation states with a variety of barriers and energies. Many of these have been analysed and that approach could be applied here³⁵⁻³⁹. The situation can also be approximated by passage over a double parabolic barrier¹⁹. In this approach, the activation enthalpy is the total of all the quantities discussed above and the entropy is a similar sum. Furthermore, the pre-exponential term is multiplied by $l_0/2l$ where l_0 is the repeat distance and l is the molecular length. For jumping over multiple barriers of equal height, the approaches are equivalent^{19,39}. The latter one is used as an approximation here.

All the results can be represented by an equation of the form:

$$D = Ae^{-B/RT} + Ce^{-E/RT} \quad (3)$$

Here D is the diffusion coefficient; A and C are pre-exponential factors; and B and E are activation enthalpies. The values given in Table 5 show that diffusion by a vacancy mechanism can certainly occur both parallel and perpendicular to the basal plane for all three subcells. In general, the greatest diffusion occurs in the triclinic subcell. Diffusion parallel to the basal plane is greater than that perpendicular to it. The activation enthalpies are all of the order of 200 kJ mol^{-1} . Subsequent to our original work, tracer diffusion measurements were reported for *n*-eicosane and stearic acid single crystals^{1,6,10}. In that work both the activation enthalpies for diffusion perpendicular to the basal plane and the pre-exponential factors are greater than these in Table 5. Nevertheless, the diffusion coefficients calculated here are in order of magnitude agreement with experimental values. A strict comparison cannot be made with the experimental diffusion parallel to the basal plane since it was dominated by pipe diffusion. It should be noted that the computed coefficients are especially sensitive to the parameters used. Among these, the values computed from equation (2) for ΔS , the value of w_0 , as well as the values of the enthalpies for perpendicular diffusion are important.

CONCLUSION

Semiempirical energy calculations have been used to study the process of self-diffusion in *n*-alkane crystals. The results show that the greatest factor in determining the diffusion coefficient is the energy associated with having a vacancy into which a molecule may move. The energy associated with the barrier to the actual molecular

motion is relatively less important. For diffusion parallel to the basal plane of the *n*-alkane crystals, self-diffusion is most likely a rigid rod motion. Diffusion normal to the basal plane must entail a conformational jog to accomplish interlayer diffusion. Diffusion coefficients for orthorhombic, monoclinic and triclinic subcells are generally similar in a particular crystallographic direction. Considering the computational approximations and the experimental difficulties involved, the calculated diffusion coefficients are in reasonable agreement with the limited experimental data available.

There are several opportunities for future work. There is a strong need for experimental diffusion coefficients for single crystals of alkanes of high purity and perfection. In order to provide the needed energies, modelling of the specific jogs for interlayer transport of the molecules should be carried out. There is an opportunity for more theoretical work on the jump kinetics of linear molecules, especially between layers. Finally there is a need to determine the excess enthalpy and entropy of vacancies experimentally using phenomena such as positron annihilation on the thermal generation of vacancies and substitutional sites^{13,40}.

REFERENCES

- Narang, R. S. and Sherwood, J. N. *Mol. Cryst. Liq. Cryst.* 1980, **59**, 167
- Chang, C. and Krimm, S. *Bull. Am. Phys. Soc.* 1980, **25**, 279
- Bloor, D., Bonsor, D. H. and Batchelder, D. N. *Mol. Phys.* 1977, **34**, 939
- Ewen, B. and Richter, D. *J. Chem. Phys.* 1978, **69**, 2954
- Richter, D. and Ewen, B. in 'Neutron Inelastic Scattering', IAEA, (1977)
- Narang, R. S. and Sherwood, J. N. *J. Mater. Sci.* 1980, **15**, 2729
- Piesczek, W., Ewen, B., Fischer, E. W. and Strobl, G. *Colloid Polym. Sci.* 1974, **252**, 896; Strobl, G., Ewen, B., Fischer, E. W. and Piesczek, W. *J. Chem. Phys.* 1974, **61**, 5257
- Ungar, G. and Keller, A. *Colloid Polym. Sci.* 1979, **257**, 90
- Zerbi, G., Piazza, R. and Holland-Moritz, K. *Polymer* 1982, **23**, 1921
- Eby, R. K. and Farmer, B. L. *Bull. Am. Phys. Soc.* 1979, **24**, 479
- Farmer, B. L. and Eby, R. K. *Bull. Am. Phys. Soc.* 1982, **27**, 296
- Farmer, B. L. and Eby, R. K. *Nuclear Metallurgy* 1976, **20**, 154
- Lightbody, D., Sherwood, J. N. and Eldrup, M. *Chem. Phys. Lett.* 1980, **70**, 487
- Meakins, R. J. *Trans. Faraday Soc.* 1959, **55**, 1694
- McCullough, R. L. *J. Macromol. Sci., Phys.* 1974, **9**, 97
- Farmer, B. L. and Eby, R. K. *J. Appl. Phys.* 1975, **46**, 4209
- Scherr, H., Hagele, P. C. and Grossman, H. P. *Colloid Polym. Sci.* 1974, **252**, 871
- Reneker, D. H., Fanconi, B. M. and Mazur, J. J. *J. Appl. Phys.* 1977, **48**, 4032

- 19 Mansfield, M. and Boyd, R. H. *J. Polym. Sci., Polym. Phys. Edn.* 1978, **16**, 1227
- 20 Farmer, B. L. and Eby, R. K. *J. Appl. Phys.* 1974, **45**, 4229
- 21 Williams, D. E. *J. Chem. Phys.* 1967, **47**, 4680
- 22 Kenny, K. H. and Heald, P. T. *Phil. Mag.* 1974, **29**, 1137
- 23 Billmeyer, F. W., Jr. *J. Appl. Phys.* 1957, **28**, 1114; Mnykh, Yu. V. *J. Phys. Chem. Solids.* 1963, **24**, 631
- 24 Smith, A. E. *J. Chem. Phys.* 1953, **21**, 2229
- 25 Shearer, H. M. M. and Vand, V. *Acta Cryst.* 1956, **9**, 379. See also Mathisen, H., Norman, N. and Pedersen, B. F. *Acta Chem. Scand.* 1967, **21**, 127
- 26 Jost, W. 'Diffusion in Solids, Liquids, Gases', Academic Press Inc., New York, 1952
- 27 Shewmon, P. G. 'Diffusion in Solids', McGraw-Hill Company, New York, San Francisco, Toronto and London, 1963
- 28 Manning, J. R. 'Diffusion Kinetics for Atoms in Crystals', D. Van Nostrand Company, Inc., Princeton, Toronto, London and Melbourne, 1968
- 29 Chadwick, A. V. and Sherwood, J. N. in 'Diffusion Processes', (Eds. J. N. Sherwood, A. V. Chadwick, W. M. Muir and F. L. Swinton), Gordon and Breach, London, New York and Paris, 1971, Vol. 2, p. 475
- 30 Eby, R. K. *J. Chem. Phys.* 1962, **37**, 2785
- 31 Seyer, W. F., Patterson, R. F. and Keays, J. L. *J. Am. Chem. Soc.* 1944, **66**, 179; Kitaigorodski, V. and Mniukh, In. V. *Sov. Phys. Dokl.* 1958, **3**, 707
- 32 Vand, V. *Acta Cryst.* 1953, **6**, 797; Müller, A. *Proc. Roy. Soc.* 1930, **A127**, 417
- 33 Cole, E. A. and Holmes, D. R. *J. Polym. Sci.* 1960, **46**, 245
- 34 Davis, G. T., Eby, R. K. and Colson, J. P. *J. Appl. Phys.* 1970, **41**, 4316
- 35 McMahon, P. E., McCullough, R. L. and Schlegel, A. A. *J. Appl. Phys.* 1967, **38**, 4123
- 36 Hoffman, J. D. and Pfeiffer, H. G. *J. Chem. Phys.* 1954, **22**, 132
- 37 Hoffman, J. D. *J. Chem. Phys.* 1955, **23**, 1331
- 38 Axilrod, B. M. *J. Res. Natl. Bur. Stand.* 1956, **56**, 81
- 39 Zwolinski, B. J., Eyring, H. and Reese, C. E. *J. Phys. Chem.* 1949, **53**, 1426
- 40 Eby, R. K. *J. Appl. Phys.* 1962, **33**, 2253